

Terahertz spectroscopy of bound water in nano suspensions

S. P. Mickan^{a,b}, J. Dordick^c, J. Munch^d, D. Abbott^b and X.-C. Zhang^a

^aCenter for Terahertz Research and Department of Physics, Applied Physics & Astronomy, Rensselaer Polytechnic Institute, Troy NY 12180, USA.

^bCentre for Biomedical Engineering (CBME) and Department of Electrical & Electronic Engineering, The University of Adelaide 5005, Australia.

^cDepartment of Chemical Engineering, Rensselaer Polytechnic Institute, Troy NY 12180, USA.

^dDepartment of Physics & Mathematical Physics, The University of Adelaide 5005, Australia.

ABSTRACT

The study of enzymatic protein molecules using terahertz time-domain spectroscopy (THz-TDS) has the potential to reveal molecular activity in real time without the use of labelling. Molecular hydration, or bound water, is a critical parameter in enzyme activity and THz-TDS measurements. For the first time we experimentally measure the terahertz-frequency response of nano-sized particles of protein and their level of molecular hydration. These measurements are valuable in understanding the terahertz response of biological systems and in studying the interaction between bound water and proteins.

Keywords: terahertz time-domain spectroscopy, ultrafast, organic solvent, FIR dielectric, bound water, 1,4-dioxane

1. INTRODUCTION

The hydration of an organic macro-molecule is a critical parameter for determining both the spectroscopic absorption and chemical activity of the molecule. Terahertz time-domain spectroscopy (THz-TDS) is a spectroscopic technique with extremely high sensitivity in the far-infrared (FIR), where macro-molecules are known to exhibit broad, conformation-dependent absorptions, and where water causes strong absorption.

1.1. Motivation

There are two primary motivations for this project. The first is to demonstrate a real-time, non-invasive and label-free method of monitoring the activity of enzymatic proteins in certain environments. The second is to study the far-infrared response of these proteins with a view to increasing our understanding of how biological macro-molecules interact with terahertz radiation. These motivations are intertwined in that the activity of enzymatic proteins in certain environments, for example in organic solvents, depends to a large extent on their molecular hydration.

Molecular activity of enzymes is dependant on protein conformation and hydration.¹ Conformation-dependant absorption changes have been observed in some biomolecules using terahertz spectroscopy,

S. P. Mickan, Email: spmickan@eleceng.adelaide.edu.au; J. Dordick, Email: dordick@rpi.edu; J. Munch, Email: jmunch@physics.adelaide.edu.au; D. Abbott, Email: dabbott@eleceng.adelaide.edu.au; X.-C. Zhang, Email: zhangxz@rpi.edu.

which suggests THz-TDS may be useful in more general observations of enzyme activity.² In microfluidic and biosensor experiments, for example, enzymatic proteins are routinely attached to the surfaces of the chip. The activity of these deposited proteins is very difficult to determine using existing spectroscopic methods. However if THz is to be used to determine the activity of proteins on surfaces, we must first develop a good understanding of the THz spectra of proteins and how influential the hydration parameter is.

Pure water has a very high absorption in the far-infrared, with an absorption coefficient of $\alpha = 100\text{--}200\text{ cm}^{-1}$ between 0.1 and 1.0 THz.³ The interaction of protein and water is interesting for monitoring activity and as a critical parameter in the FIR study of biomolecules. However, the high absorption of an aqueous environment makes it difficult to observe small changes in protein hydration. In our study, we use anhydrous organic solvents to suspend the protein molecules, enabling us to experimentally control the hydration level with great accuracy. Depending on concentration levels, the protein forms nano-sized clumps, suspended in the solvent, and water binds to the protein, depending on the available hydration. Bound water studies are extremely valuable in biological reactions. Previous studies using the sensitive THz spectrometer have observed water binding to ionic salts.⁴

1.2. Previous studies

Biological systems are overwhelmingly water-based but the high absorption of water makes it difficult to conduct experimental studies of proteins in their native environments. Previous biomolecule studies have used dried pellets and thin film samples.^{5,6} These systems have allowed careful control of pressure, temperature and humidity, but it is difficult to conduct real-time chemical reactions using solids.

In certain organic solvent suspensions, biomolecules have been shown to retain their activity and it will be possible to monitor chemical interactions in real time with THz-TDS.

2. EXPERIMENTS

All samples are prepared with off-the-shelf chemical and biological materials. All spectroscopic experiments are conducted with a fairly typical custom-built THz spectrometer, based around ultrafast electrooptic THz pulse generation and detection. The spectroscopic responses of the samples are analysed in terms of their complex refractive index.

2.1. Sample preparation

The three important materials in our experiments are an organic solvent, protein molecules and pure water. Deionised, doubly-distilled water is routinely obtained from a Millipore *RiOs* purification system.

Protein activity studies have been conducted in a range of organic solvents, showing a dependence on solvent dielectric constant, temperature, ionic salts and hydration.⁷ For THz spectroscopy, we require a solvent that has a very low THz absorption, thus a solvent that is largely non-polar. Unfortunately, most non-polar solvents are poorly water-miscible, which limits the range of protein hydration available. 1,4-dioxane, however, is a non-polar solvent with high water miscibility. A 1,4-dioxane molecule is charge symmetric, so has a small electrical dipole, but the two OH-groups enable the integration of water molecules into the dioxane matrix. The 1,4-dioxane molecule is shown in Fig. 2.1. We refer to 1,4-dioxane in this paper as dioxane. Dioxane was purchased from Aldrich, 99.8% anhydrous, CAS no. 123-91-1, lot no. 29630-9, and stored over Fisher 3-Å molecular sieves for >24 hrs to maintain low hydration.

There are many biologically important and easily-available proteins commonly used to study enzyme activity and protein hydration. In this experiment, we use the protein *subtilisin Carlsberg* (SC),

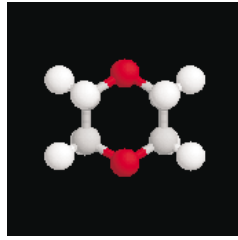


Figure 1. Diagrammatic representation of the 1,4-dioxane molecule. The symmetric nature of the molecule is visible, which causes its weak permanent dipole moment. The dark spheres represent OH groups, which readily form hydrogen bonds with water, giving it a very high water miscibility, unlike other non-polar liquids.

as it is known to demonstrate changes in activity for small changes in molecular hydration and because the water shell bound to SC has been previously documented.⁸ SC was purchased from Sigma, CAS no. 9014-01-1, lot no. 91K1107, and used without further purification. The SC was buffered in doubly-distilled water and lyophilised for >24 hrs, then immediately suspended in dioxane. SC has a tendency to settle out of suspension in dioxane, so all mixtures were thoroughly sonicated directly prior to spectroscopic measurement.

The five mixtures of interest are listed in Table 1. Pure dioxane is studied at different levels of hydration for normalization purposes. In this case, dioxane is characterised while anhydrous (water content <0.003%) and hydrated (water content 0.2%). The addition of protein to the dehydrated and hydrated solvents shows a shift in the complex THz refractive index of each mixture, and this shift depends on the fraction of free water present in the mixture. The shift in refractive index caused by the protein can be compared to the refractive index of the solvent to determine the properties of the protein molecules with different hydrations. The final mixture is prepared by adding SC to the hydrated dioxane, then removing the SC via centrifuge, leaving only the supernatant. The refractive index of the supernatant shows how much of the water present in the hydrated solvent is attached to the SC molecules. The meaning of these results is discussed in detail in Sect. 3.

Table 1. Mixtures used in the experiments. Volume measurements are accurate to 5% using pipettes. The ‘?’ in mix 5 indicates that the volume of water remaining in the mixture is dependant on the water binding affinity of the SC; mix 5 is prepared by centrifuging the suspended protein from mix 4, which removes a portion of the water found in mix 4.

| Mixture | Dioxane | Water | SC |
|---------|---------|------------|-------|
| mix 1 | 10 mL | - | - |
| mix 2 | 10 mL | - | 20 mg |
| mix 3 | 10 mL | 20 μ L | - |
| mix 4 | 10 mL | 20 μ L | 20 mg |
| mix 5 | 10 mL | ? | - |

2.2. THz Time-Domain Spectrometer

The THz generation and detection system used in this experiment has been described elsewhere.⁹ FIR or THz radiation can be generated and detected using a large variety of continuous and pulsed devices and techniques.¹⁰ However, these sources and detectors have various short-comings, leaving a ‘THz gap’ in the electro-magnetic spectrum. Only recently, with the demonstration of the THz quantum cascade laser, has the leap to electrically-pumped solid-state sources been made.¹¹ Pulsed THz radiation has a very low average power, making it harmless, and is detected with a very high sensitivity, resulting in a large signal-to-noise ratio (SNR) for experiments in the FIR.

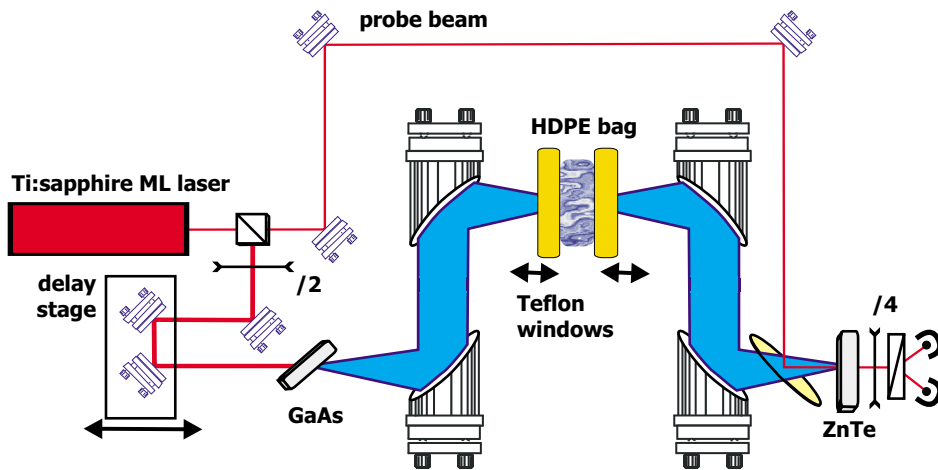


Figure 2. Typical THz spectrometer configured for dual-thickness liquid spectroscopy. The Ti:sapphire mode-locked (ML) laser generates a train of 100-fs pulses at 82 MHz. Each pulse is split into a pump beam and a probe beam. The pump beam generates THz pulses when incident at Brewster's Angle on the GaAs wafer, positioned at the focal point of a gold-coated parabolic reflector. Parabolic reflectors collimate the THz, focus it into the sample holder, then collect the transmitted radiation and direct it into a $\langle 110 \rangle$ ZnTe THz detector. The probe beam detects the THz electric field in the ZnTe, and is in turn recorded with crossed polarisers and balanced photodetectors. The thickness of the sample is modulated with two Teflon windows, one of which is mounted on manual translation stage. The mixture is held in a sealed, thin-walled, high-density polyethylene (HDPE) bag, which is resistant to dioxane.

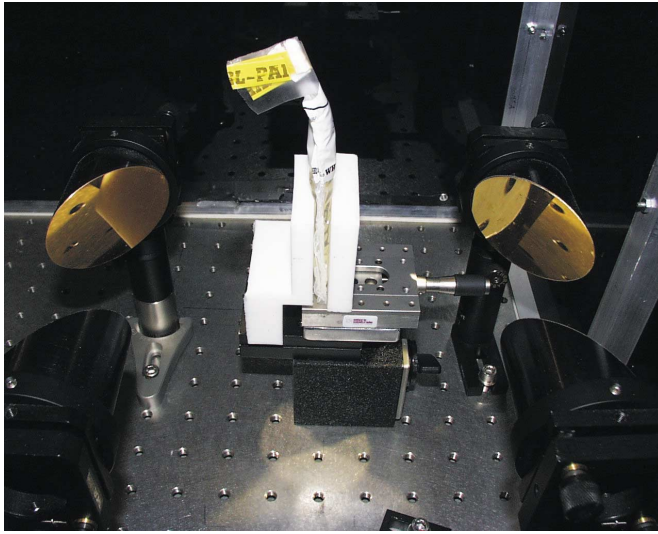
The fluid sample to be studied is held in a variable path-length liquid sample holder, based on a design by Schmuttenmaer.¹² The sample is contained in a sealed high-density polyethylene sample bag with a wall thickness $\approx 60 \mu\text{m}$. The thickness of the sample is controlled by two 10-mm-thick Teflon windows, placed parallel to each other and perpendicular to the beam path. Teflon is chosen for its price, machinability, low THz absorption and low THz refractive index. All spectroscopic measurements require the sampling of two waveforms, a sample waveform y_s and a reference waveform y_r . The sample waveform is radiation that has passed through a thick sample, thickness d_s , and the reference waveform is from a thin sample, d_r , shown in Fig. 2.4. The sample thickness is varied by a manual stage, which translates one of the windows of the sample holder along the axis of the beam path.

2.3. Environmental conditions

The THz free path section of the THz spectrometer is enclosed in a sealed, air-tight box to block air movement which would disturb the pellicle beam splitter. The experiments were conducted at room temperature, held by air conditioning to about 20°C , and at a relative humidity of approximately 40%.

2.4. Fluid parameter estimation

The THz absorption of each mixture is calculated through plane wave calculations. The THz pulse is modelled as a spectrum of Fourier components, propagating as a plane wave through the sample. Figure 2.4 shows the propagation of radiation through the sample, of complex refractive index \tilde{n}_2 , and across two interfaces between the sample and the surrounding medium (air), $\tilde{n}_1 \approx 1.0$. The simple equations used for estimating the material parameters are derived from the equations for Fresnel transmission and reflection at interfaces as follows.^{13, 14}



(a) Variable-thickness sample holder



(b) Liquid sample in HDPE bag

Figure 3. Details of the liquid sample holder. The variable-length holder is shown at the focal point of the focusing and collection optics. The thickness of the Teflon windows is >10 -mm to avoid any Fabry-Pérot (FP) reflections within our timing window. The thickness of the sample is modulated from a minimum of 3-mm, chosen to avoid FP reflections, to a maximum of 7-mm, the maximum possible with this liquid volume that ensures a complete coverage of the THz beam path. A large thickness change is desirable to minimise the uncertainty in our parameter estimations.

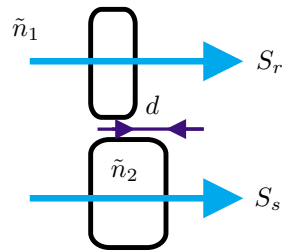


Figure 4. Geometry used in dual-thickness parameter estimation. Waveforms y_s and y_r are measured having respectively passed through the thick (sample) and thin (reference) samples. The spectral components of the waveforms are determined by FFT, $S_s = \mathcal{FT}(y_s)$ and $S_r = \mathcal{FT}(y_r)$. The difference in thickness between the two measurements is denoted d .

The spectral components of an electric field after propagating through a sample \tilde{n}_2 , of thickness d_2 , can be expressed as

$$S(\omega) = \eta(\omega) \frac{2\tilde{n}_1}{\tilde{n}_1 + \tilde{n}_2} e^{-j\tilde{n}_2\omega d_2/c_0} \frac{2\tilde{n}_2}{\tilde{n}_2 + \tilde{n}_1} \text{FP}(\omega) E(\omega), \quad (1)$$

where $E(\omega)$ is the field emitted by the THz source, $\text{FP}(\omega)$ accounts for Fabry-Pérot reflections in the sample. $\eta(\omega)$ accounts for effects of the system between the sample and the THz emitter and detector. $\eta(\omega)$ is constant for any sample for thickness d_2 . For a sufficiently thick sample, as used in this experiment, there are no FP reflections, so $\text{FP}(\omega) = 1$.

For two samples of the same material, identical except for thickness, the transmission spectrum of the pure material can be obtained by taking the ratio of the two spectra: all the interface effects are

cancelled out and only the propagation effects remain, which are simple to model. The transmission ratio is expressed as

$$T = S_{\text{sample}}/S_{\text{reference}} = \frac{e^{-j\tilde{n}_2\omega d_{\text{sample}}/c_0}}{e^{-j\tilde{n}_2\omega d_{\text{reference}}/c_0} e^{-j\tilde{n}_1\omega(d_{\text{sample}}-d_{\text{reference}})/c_0}}, \quad (2)$$

where \tilde{n}_1 is the material that replaces the space taken up by the extra thickness of the thick sample, typically air.

Equation 2 simplifies to

$$T = \exp(-j\omega/c_0 d(\tilde{n}_2 - 1)), \quad (3)$$

where $d = d_{\text{sample}} - d_{\text{reference}}$ and $\tilde{n}_1 = 1$. Since T is complex, $T = \rho e^{j\phi}$, and $\tilde{n} = n - j\kappa$,

$$\rho = \exp(-\omega d \kappa / c_0), \quad (4)$$

and

$$\phi = \omega \Delta d (n_2 - 1) / c_0. \quad (5)$$

The material parameters can then be extracted by rearranging the equations above,

$$n = \frac{-\phi c_0}{\omega d} + 1, \quad (6)$$

$$\kappa = -\ln(\rho) \frac{c_0}{\omega d}. \quad (7)$$

These calculations provide a value for the THz refractive index and extinction of the mixture. The uncertainty in our preliminary measurements is estimated from the standard deviation of separate measurements of y_s and y_r . Future characterisations are required using a greater number of samples to increase our confidence limits.

3. RESULTS

The results of our experiments are expressed as absorption spectra, Figs. 6 and 8 for the 5 mixtures in Table 1. The bandwidth of our measurements is limited by the THz spectrometer to approximately 0.2–1.1 THz; this is the region of highest SNR, as required for accurate measurements. The bandwidth of our system can be seen in Fig. 5, which shows the spectrum of a sample waveform having passed through anhydrous 1,4-dioxane, mix 1. Visible in the sample spectrum are absorption lines due to atmospheric water vapour – these lines are present in both the sample and reference spectra, and are normalised out in the parameter estimation Eq. 2. The absorption lines increase the uncertainty of measurements at those specific frequencies; they can be avoided by purging the experimental chamber with dry nitrogen or by using an enclosed THz spectrometer.¹⁶

The absorption spectra of our mixtures in the range 0.2 – 1.1 THz at room temperature are not expected to show any specific resonance absorption lines, as are found in gas vapour samples¹⁵ or in biomolecules at lower temperatures and higher frequencies.¹⁷ Typically, liquid samples do not show specific absorption lines at THz frequencies because the roto-translational bands are so closely spaced and the overall absorption is so high.¹⁸ The biomolecules of SC in our suspensions have many randomly-oriented dipoles, which largely cancel out, and the protein cannot rotate at THz frequencies, so only atomic and electrical polarisation play a part, resulting in a dielectric constant far less than water.¹⁹ An explanation of the fine structure of the spectra cannot be achieved before the samples are studied over a broader frequency band, and with a wide variation in temperature and concentration. In our analysis, we are interested in the broad, dielectric-constant-like absorption increase and decrease of our mixtures.

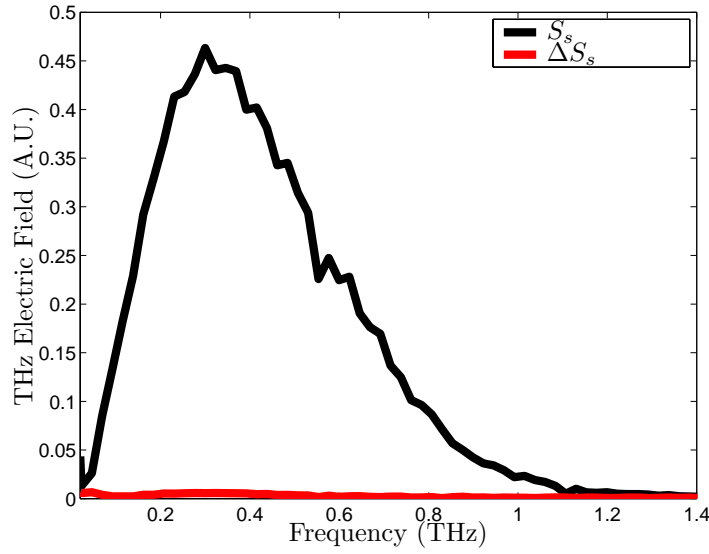


Figure 5. Spectral components of the mean of 6 sample THz waveforms, S_s , through mix 1. The thick plot (S_s) is the FFT of the sample waveform. The grey plot (ΔS_s) is the standard deviation over 6 waveforms. The thickness of the plots represents this uncertainty. This figure demonstrates the bandwidth of good SNR for our spectrometer and shows absorption lines due to atmospheric water (at 0.56, 0.75 and 1.1 THz).¹⁵

3.1. Dioxane & water

Mixtures of dioxane and water have been studied with microwave spectroscopy, and characterised with Debye models.²⁰⁻²³ Our estimation of the absorption of anhydrous dioxane, mix 1 in Table 1, is shown as a thick black line in Fig. 6. As discussed in the introduction, dioxane has a low absorption in the THz range, far less than polar liquids, for example water, and only slightly greater than highly non-polar liquids, including toluene and hexane.^{24, 25} The thickness of the plot indicates the uncertainty in our estimations.

The addition of 2 $\mu\text{L}/\text{mL}$ of pure water to the dioxane greatly increases the absorption of the mixture, mix 3 in Table 1. The absorption of mix 3 is shown as a grey line with black points in Fig. 6. The absorption spectrum of mix 3 is clearly greater than mix 1, caused by the addition of polar water molecules to the essentially non-polar dioxane matrix.

The dioxane-water mixture can be compared to a mix of ideal liquids, where the mixture absorption would be given by the relation

$$\kappa_{\text{mix 3 (ideal)}} = v_w \kappa_{\text{water}} + v_d \kappa_{\text{dioxane}}, \quad (8)$$

where v_w and v_d are respectively the partial volume fractions of water and dioxane.²⁶ The predicted absorption of an ideal mixture of 2 $\mu\text{L}/\text{mL}$ of water in dioxane is shown as a grey plot in Fig. 7. This ideal mixture demonstrates an increased absorption, but not as large as the measured absorption of mix 3, shown as black dots in Fig. 7. This quantitative mismatch is caused by the non-ideal mixing of water and dioxane; the addition of water to dioxane requires the use of extra relaxation terms in a Debye model of the mixture at microwave frequencies. Nevertheless, it is instructive to note that the altered trend of the spectral curve, from having a positive to having a negative slope, could be explained in part by an ideal water-dioxane mixture with a higher water concentration (15 $\mu\text{L}/\text{mL}$), shown as a grey line with black dots in Fig. 7.

The water absorption spectrum used to estimate the ideal liquid absorption in Fig. 7 was calculated

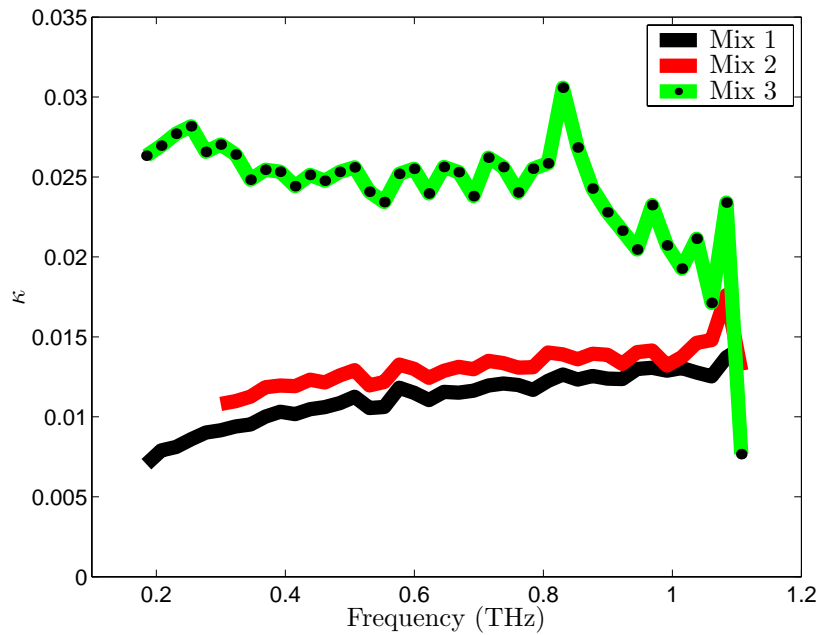


Figure 6. Absorption spectra of the first 3 mixtures from Table 1. The bandwidth is limited to the region of maximum SNR. The plots show the mean of 6 measurements, and the plot thickness indicates the standard deviation of those measurements. The broad features are of interest, since characterisation of small-scale features at THz frequencies is difficult. Mix 1 is anhydrous dioxane. Mix 2 is dioxane and SC, and shows a very slight increase in absorption, if at all (the plots overlap in points). Mix 3, hydrated dioxane, shows a marked increase in absorption, due to the increased polarity caused by adding strongly polar water molecules.

from the double Debye model of pure water published by Keiding.²⁷ Keiding's water model was based on their experimental THz data and later corroborated by Koch.²⁸

The THz absorption of a dioxane mixture including water must be compared to the absorption of a dioxane mixture with SC (mix 2) to eventually quantify the interaction between the biomolecules and the water.

3.2. Subtilisin *Carlsberg*

The THz absorption of biological macro-molecules has been measured⁶ to be in the region $\alpha \approx 60 \text{ cm}^{-1}$. Protein absorption is low because the majority of dipoles cancel out, although the molecules do retain some polarity so their absorption is slightly higher than the anhydrous dioxane. The THz absorption spectrum of the dioxane-SC mixture, mix 2, is shown as a grey plot in Fig. 6, indicating only a slight increase in absorption over the anhydrous dioxane. These measurements indicate two important results: that the dielectric constant of the lyophilized protein is greater than anhydrous dioxane, and that the increased absorption of 2 mg/mL of SC in dioxane is slight (less than 10%).

For 2 mg/mL of SC in dioxane, the absorption of mix 2 can be modelled as an ideal mixture if $\alpha_{\text{SC}} < 200 \text{ cm}^{-1}$. Although the ideal model is incorrect, it indicates a probable maximum absorption for SC at THz frequencies.

3.3. Free & bound water

Protein molecules operate natively in water-rich environments, and the binding of water molecules to the protein surface is a critical process in understanding activity and interaction of protein systems. The hydration shell of a protein molecule has been described as a tightly-bound layer of low-mobility

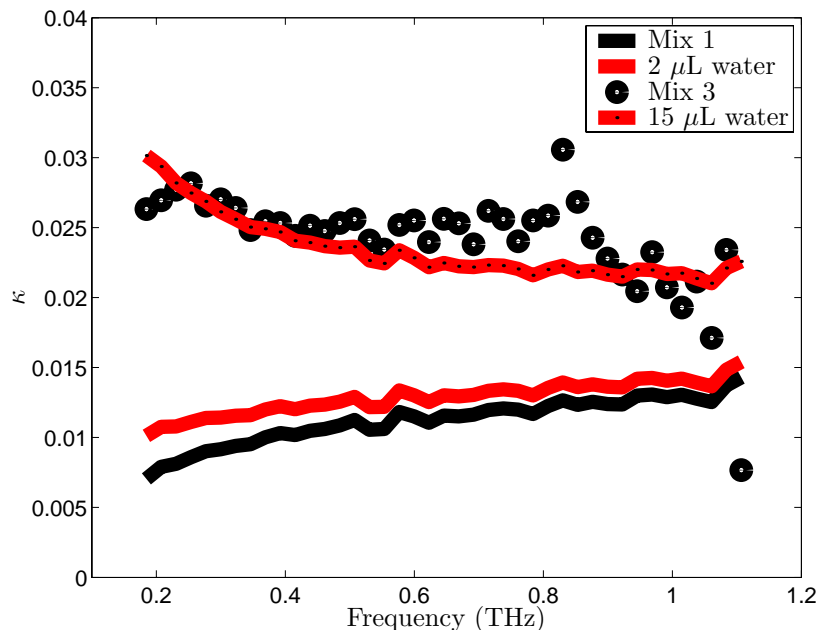


Figure 7. Calculated absorption spectrum of mix 3, hydrated dioxane, assuming ideal liquids (mixing by volume fraction), for two added water volumes. For the experimental value, $2 \mu\text{L}/\text{mL}$ of water in dioxane, a slight increase in absorption is visible. This is, however, less than the experimentally-observed increase in absorption (mix 3) since the ideal mixing model is incorrect, as shown in microwave experiments. The trend, however, is clear – higher absorption. This trend can be further explored by artificially increasing the volume fraction of water in our model, to give the plot for dioxane plus $15 \mu\text{L}/\text{mL}$ water. This artificial plot shows that the changed slope of absorption from mix 1 to mix 3 could be attributed to the water absorption curve. Water absorption was estimated from the Debye model of Keiding.²⁷

water molecules, surrounded in turn by free water molecules in the liquid matrix.²⁹ The two types of water, free water and bound water, exhibit different dielectric constants. Free water interacts with incident radiation similarly to bulk water, having a high dielectric constant (≈ 80). The dipole of bound water is hindered in its motion and has a far lower dielectric constant. Our measurements of the water-protein mixture, suspended in dioxane, can be explained by the model of bound and free water.

Figure 8 shows the central result of this paper, that the addition of SC to a mixture of dioxane and water lowers the dielectric constant of the mixture. Hydrated dioxane, mix 3, is shown as a grey line with black dots in Fig. 8, and the mixture of dioxane, water and SC is a solid black line. Without the consideration of water binding to the lyophilised SC molecules, the addition of a small volume fraction of SC should make no difference to the absorption spectrum of the mixture. For $2 \text{ mg}/\text{mL}$ of SC in $2 \mu\text{L}/\text{mL}$ water-dioxane (mix 5) the volume fraction of SC is 0.2%. The observed decrease cannot to be due to volume displacement effects alone because the volume of SC is so small.

The percentage of the free water present in mix 3 that is bound to the introduced SC molecules in mix 4 can be estimated from previous measurements of the hydration shell of SC; it is estimated that there are 500 bound water molecules per SC, approximately 400 of which are removed by lyophilisation.⁸ From molar calculations, the number of SC molecules present in mix 2 equals $75 \text{ nM}/\text{mL}$, which corresponds to approximately $30 \mu\text{M}/\text{mL}$ of water being bound to the added lyophilised SC. The moles of water present in mix 3 $\approx 110 \mu\text{M}/\text{mL}$, predicting a decrease in the free water absorption increment of approximately 27%. The water absorption increment in Fig. 8 is decreased by about

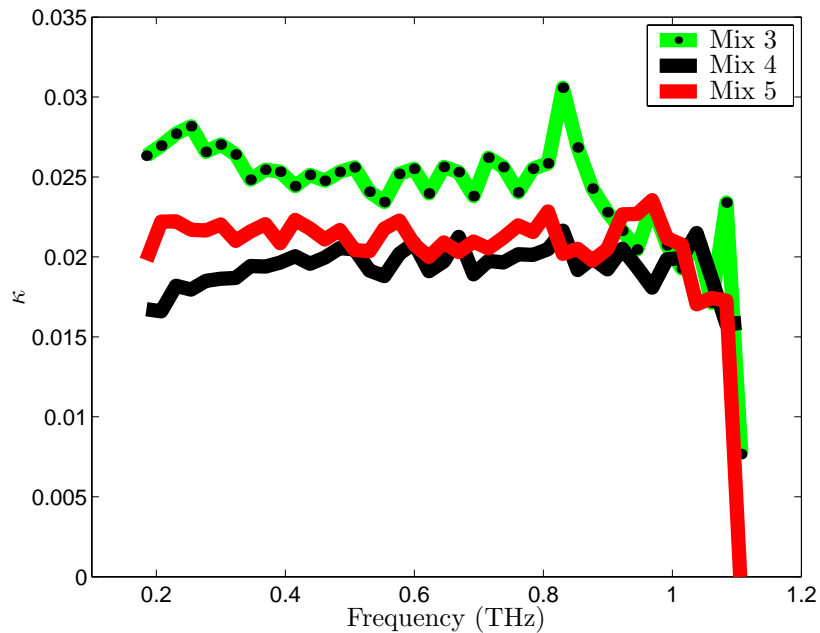


Figure 8. Absorption spectra of the last 3 mixtures from Table 1. The bandwidth is limited to the region of maximum SNR. The plots show the mean of 6 measurements, and the plot thickness indicates the standard deviation of those measurements. The broad features are of interest, since characterisation of small-scale features at THz frequencies is difficult. Mix 3 is hydrated dioxane, as in Fig. 6. Mix 4 includes SC with the hydrated dioxane and shows a markedly reduced absorption. Mix 5 was prepared by physically removing SC, and the water bound to it. Mix 5 has approximately the same absorption as mix 4, showing that the reduction in absorption from mix 3 to mix 4 is due to an interaction between SC and the mixture, not just to the SC.

30%–40% with the addition of SC, depending on frequency. These results can be explained by assuming that a measurable portion of the free water molecules responsible for the absorption of mix 3 are bound to the SC in mix 4.

The assumption of free water binding to the SC in mix 4 can be tested by physically removing the protein. The SC is filtered out with a centrifuge, leaving only the liquid phase as mix 5. Mix 5 contains dioxane and free water, as bound water has been removed with the protein. The absorption of mix 5 is almost identical to the absorption of mix 4 and discernably less than mix 3, as shown in Fig. 8. The fact that the absorption of mix 5 is lower than mix 3 shows that the SC molecules have interacted irreversibly with the mixture, and acted to reduce the overall absorption spectrum. This can be well explained by the bound water model. The slight increase in absorption from mix 4 to mix 5 may be due to the slight increase in volume fraction of the free water as the protein and bound water is removed.

The estimated volume fractions of the 5 mixtures are presented in Table 2, including possible numbers for free and bound water in mix 4 and mix 5.

4. CONCLUSIONS & FUTURE WORK

We have conducted THz absorption experiments for the first time on protein suspensions in organic solvents. The high water miscibility of the non-polar solvent dioxane was used to conduct well-controlled hydration measurements on the protein subtilisin *Carlsberg*. The bandwidth of the THz spectrometer provided access to the under-explored THz region of the electromagnetic spectrum, a region where water absorption is high and research indicates the possibility of conformation-dependant

Table 2. Volume fractions (%) for mixtures of 1-mL anhydrous dioxane, 2- μ L pure water and 2-mg lyophilised SC.

| Mixture | Dioxane | Water | | SC |
|---------|---------|-------|-------|-----|
| | | Free | Bound | |
| mix 1 | 100.0 | - | - | - |
| mix 2 | 99.8 | - | - | 0.2 |
| mix 3 | 99.8 | 0.2 | - | - |
| mix 4 | 99.6 | 0.1 | 0.1 | 0.2 |
| mix 4 | 99.9 | 0.1 | - | - |

biomolecular resonances.^{5,30,31} We observed the dielectric constant of free water and water bound to the suspended protein.

The dioxane environment provides a way to study biomolecules in THz transmission, where hydration and temperature can be carefully controlled and real-time chemical reactions can conceivably be carried out. THz can non-invasively estimate the activity of enzymatic proteins, used for example in micro-flow reactors, by measuring water content with high sensitivity.

In future work we intend to reduce the uncertainty in our estimations and provide molecular-level models of these results. Numerical modelling is the best way to understand the interaction of liquids and biomolecules at a molecular level.^{17,32,33} The uncertainty in our liquid measurements will be increased by the implementation of a *differential* sampling technique in our THz spectrometer.^{34,35} This will lead to more quantitative measurements of solvents and protein absorption in the THz band.

ACKNOWLEDGMENTS

The authors would like to acknowledge the experimental assistance of Chris Kona and Regina Shvartsman, and financial support from the US National Science Foundation, the US Army Research Office, the Australian Fulbright Commission and the Australian Research Council.

REFERENCES

1. J. Partridge, P. R. Dennison, B. D. Moore, and P. J. Halling, "Activity and mobility of subtilisin in low water organic media: hydration is more important than solvent dielectric," *Biochimica et Biophysica Acta* **1386**, pp. 79–89, 1998.
2. M. Walther, B. Fischer, M. Schall, H. Helm, and P. U. Jepsen, "Far-infrared vibrational spectra of all-trans, 9-cis and 13-cis retinal measured by THz time-domain spectroscopy," *Chemical Physics Letters* **332**(3–4), pp. 389–95, 2000.
3. L. Thrane, R. H. Jacobsen, P. U. Jepsen, and S. R. Keiding, "THz reflection spectroscopy of liquid water," *Chemical Physics Letters* **240**, pp. 330–333, 1995.
4. M. L. T. Asaki, A. Redondo, T. A. Zawodzinski, and A. J. Taylor, "Dielectric relaxation of electrolyte solutions using terahertz transmission spectroscopy," *Journal of Chemical Physics* **116**(19), pp. 8469–8482, 2002.
5. M. Brucherseifer, M. Nagel, P. Haring Bolívar, H. Kurz, A. Bosserhoff, and R. Büttner, "Label-free probing of the binding state of DNA by time-domain terahertz sensing," *Applied Physics Letters* **77**(24), pp. 4049–4051, 2000.
6. A. G. Markelz, A. Roitberg, and E. J. Heilweil, "Pulsed terahertz spectroscopy of DNA, bovine serum albumin and collagen between 0.1 and 2.0 THz," *Chemical Physics Letters* **320**(1–2), pp. 42–48, 2000.

7. M. T. Ru, K. C. Wu, J. P. Lindsay, J. S. Dordick, J. A. Reimer, and D. S. Clark, "Towards more active biocatalysts in organic media: Increasing the activity of salt-activated enzymes," *Biotechnology and Bioengineering* **75**(2), pp. 187–196, 2001.
8. S. K. Pal, J. Peon, and A. H. Zewail, "Biological water at the protein surface: Dynamical solvation probed directly with femtosecond resolution," *Proceedings of the National Academy of Sciences* **99**(4), pp. 1763–1768, 2002. doi/10.1073/pnas.042697899.
9. S. P. Mickan, K. S. Lee, T.-M. Lu, J. Munch, D. Abbott, and X.-C. Zhang, "Double modulated differential THz-TDS for thin film dielectric characterization," *Microelectronics Journal* **In Press**, 2002.
10. S. P. Mickan and X.-C. Zhang, "Optoelectronics for terahertz wave sensing and imaging," in *Sensing Science and Electronic Technology at THz Frequencies*, D. Woolard, M. S. Shur, and W. Leorop, eds., Word Scientific Publishing Company, 2003. Accepted.
11. R. Köhler, A. Tredicucci, F. Beltram, H. E. Beere, E. H. Linfield, A. G. Davies, D. A. Ritchie, R. C. Iotti, and F. Rossi, "Terahertz semiconductor-heterostructure laser," *Nature* **417**(6885), pp. 156–159, 2002.
12. J. T. Kindt and C. A. Schmuttenmaer, "Far-infrared dielectric properties of polar liquids probed by femtosecond terahertz pulse spectroscopy," *Journal of Physical Chemistry* **100**(24), pp. 10373–10379, 1996.
13. M. Born and E. Wolf, *Principles of Optics*, Cambridge University Press, 7th ed., 1999.
14. L. DuVillaret, F. Garet, and J.-L. Coutaz, "A reliable method for extraction of material parameters in terahertz time-domain spectroscopy," *IEEE Journal of Selected Topics in Quantum Electronics* **2**(3), pp. 739–746, 1996.
15. M. van Exter, C. Fattinger, and D. Grischkowsky, "Terahertz time-domain spectroscopy of water vapor," *Optics Letters* **14**(20), pp. 1128–1130, 1989.
16. S. P. Mickan, D. Abbott, J. Munch, and X. C. Zhang, "Chemical sensing in the submillimeter wave regime," in *Smart Structures and Devices 2000*, vol. 4235, SPIE, 2000.
17. M. Walther, P. Plochocka, B. Fischer, H. Helm, and P. U. Jepsen, "Collective vibrational modes in biological molecules investigated by terahertz time-domain spectroscopy," *Biopolymers* **67**(4–5), pp. 310–313, 2002.
18. J. R. Birch, K. F. Ping, S. K. Husain, J. Yarwood, and B. Catlow, "Upper bounds for discrete features in the far-infrared spectrum of liquid acetonitrile," *Chemical Physics Letters* **117**(3), pp. 197–202, 1985.
19. R. Pethig and D. B. Kell, "The passive electrical properties of biological systems: Their significance in physiology, biophysics and biotechnology," *Physics in Medicine and Biology* **32**(8), pp. 933–970, 1987.
20. F. E. Critchfield, J. A. Gibson, Jr., and J. L. Hall, "Dielectric constant for the dioxane-water system from 20 to 35°," *Journal of the American Chemical Society* **75**, pp. 1991–1992, 1953.
21. J. Crossley and C. P. Smith, "Dielectric behavior of dilute solutions of water in *p*-dioxane," *Journal of Chemical Physics* **50**(5), pp. 2259–2260, 1969.
22. C. J. Clemett, E. Forest, and C. P. Smyth, "Microwave absorption and molecular structure in liquids. LVI. dielectric behavior of water and heavy water in dioxane," *Journal of Chemical Physics* **40**(8), pp. 2123–2128, 1964.
23. S. Mashimo, N. Miura, T. Umehara, S. Yagihara, and K. Higasi, "The structure of water and methanol in *p*-dioxane as determined by microwave dielectric spectroscopy," *Journal of Chemical Physics* **96**(9), pp. 6358–66361, 1992.
24. S. P. Mickan, J. S. Dordick, J. Munch, D. Abbott, and X.-C. Zhang, "Pulsed THz protein spectroscopy in organic solvents," in *Conference on Lasers and Electro-Optics '02*, p. 640, IEEE LEOS & OSA, (Long Beach, CA, U.S.A.), 2002.
25. J. E. Pedersen and S. R. Keiding, "THz time-domain spectroscopy of nonpolar liquids," *IEEE Journal of Quantum Electronics* **28**(10), pp. 2518–2522, 1992.

26. D. S. Venables, A. Chiu, and C. A. Schmuttenmaer, "Structure and dynamics of nonaqueous mixtures of dipolar liquids. I. Infrared and far-infrared spectroscopy," *Journal of Chemical Physics* **113**(8), pp. 3243–3248, 2000.
27. C. Rønne, L. Thrane, P.-O. Åstrand, A. Wallqvist, K. V. Mikkelsen, and S. R. Keiding, "Investigation of the temperature dependence of dielectric relaxation in liquid water by THz reflection spectroscopy and molecular dynamics simulation," *Journal of Chemical Physics* **107**(14), pp. 5319–5331, 1997.
28. M. Koch, I. H. Libon, M. Hempel, S. Seitz, N. E. Hecker, J. Feldmann, D. Mittlemen, F. Bartl, A. Hayd, and G. Zundel, "THz spectroscopy on polar liquids," in *International Conference on Lasers 1998*, V. J. Corcoran and T. A. Goldman, eds., pp. 225–231, The Society for Optical & Quantum Electronics, (Tucson, AZ, USA), 1999.
29. N. Nandi and B. Bagchi, "Dielectric relaxation of biological water," *Journal of Physical Chemistry B* **101**(50), pp. 10954–10961, 1997. DOI 10.1021/jp971879g.
30. M. Nagel, P. Haring Bolívar, M. Brucherseifer, H. Kurz, A. Bosserhoff, and R. Büttner, "Integrated planar terahertz resonators for femtomolar sensitivity label-free detection of DNA hybridization," *Applied Optics* **41**(10), pp. 2074–2078, 2002.
31. M. Nagel, P. Haring Bolívar, M. Brucherseifer, H. Kurz, A. Bosserhoff, and R. Büttner, "Integrated THz technology for label-free genetic diagnostics," *Applied Physics Letters* **80**(1), pp. 154–156, 2002.
32. D. S. Venables and C. A. Schmuttenmaer, "Structure and dynamics of nonaqueous mixtures of dipolar liquids. II. Molecular dynamics simulations," *Journal of Chemical Physics* **113**(8), pp. 3249–3260, 2000.
33. S. Hayward and N. Go, "Collective variable description of native protein dynamics," *Annual Review of Physical Chemistry* **46**, pp. 223–50, 1995.
34. Z. Jiang, M. Li, and X.-C. Zhang, "Dielectric constant measurement of thin films by differential time-domain spectroscopy," *Applied Physics Letters* **76**(22), pp. 3221–3223, 2000.
35. S. P. Mikan, D. Abbott, J. Munch, and X. C. Zhang, "Noise reduction in terahertz thin film measurements using a double modulated differential technique," *Fluctuation and Noise Letters* **2**(1), pp. 13–29, 2002.